Journal of Geochemical Exploration 166 (2016) 33–44

Contents lists available at ScienceDirect

Journal of Geochemical Exploration

journal homepage: www.elsevier.com/locate/gexplo

Coal quality characterization and its relationship with geological process of the Early Permian Huainan coal deposits, southern North China

Biao Fu [a,b], Guijian Liu [a,b,*], Yuan Liu [a], Siwei Cheng [a], Cuicui Qi [a], Ruoyu Sun [a]

[a] CAS Key Laboratory of Crust–Mantle Materials and Environment, School of Earth and Space Sciences, University of Science and Technology of China, Hefei, Anhui 230026, China
[b] State Key Laboratory of Loess and Quaternary Geology, Institute of Earth Environment, The Chinese Academy of Sciences, Xi'an, Shaanxi 710075, China

ARTICLE INFO

Article history:
Received 21 December 2015
Revised 14 March 2016
Accepted 9 April 2016
Available online 16 April 2016

Keywords:
Coal quality
Trace elements
Basin subsidence
Accommodation
Geochemistry
Huainan coalfield

ABSTRACT

The Huainan coalfield situated in the southern margin of North China Plate contains coal deposits of Carboniferous–Permian age. The 1 and 3 seams of the Early Permian Shanxi Formation and seams 4-1, 4-2, 5-1, 7-2 and 8 of the Late Early Permian Lower Shihezi Formation were analyzed for coal petrography, mineralogy and geochemical parameters. Collected data were designed to offer basic information on the assessment of coal quality and further to reveal possible factors controlling on coal quality. The shift of basin subsidence center from Huaibei coal-bearing basin to Huainan coal accumulation region caused the change of coal-forming environment (groundwater table, detrital matters and swamp style) which may further cause the differences in coal quality. The average vitrinite contents, ash yields and mineral matters are higher in the Lower Shihezi Formation coals than in the Shanxi Formation coals. The contents of vitrinite sharply decrease upward within coal seam 4, whereas the inertinite contents, ash yields and mineral matters show opposite trend which may be attributed to the relatively high-accommodation settings produce coals usually in the form of an upward high-to-low vitrinite succession. Two groups of elements are classified among coal seams. According to the vertical variation of elements contents among coal seams, most of elements in Group 1 are depleted in coal seam 4-2 except for Be, B, Sc, Fe, Mg, Ca, Li, Sn while almost all the elements in Group 2 are enriched in coal seam 4-2.

1. Introduction

Coal will continue to be a major energy source in China as well as in many other developing countries (Dai et al., 2012a; Liu et al., 2005). By the end of 2014, China has produced and consumed nearly 2 billion tons of oil-equivalent coal, ~50% of world coal production and consumption (BP report: bp.com/statisticalreview).

In recent decades, trace element releases during coal exploitation and utilization have drawn much more attention, due to their adverse impacts on the ecological environment and human health (Chen et al., 2011; Dai et al., 2008; Dai et al., 2012a, 2012b, 2012c; Liu et al., 2004; Liu et al., 2007b; Qi et al., 2011). In some local areas of China, severe endemics such as arsenosis, fluorosis, and selenosis prevail, which are presumably related to the emissions of toxic elements (As, F, Se) during burning of local coals (Dai et al., 2012a; Finkelman et al., 1999; Finkelman et al., 2002; Li et al., 2012; Liu et al., 2007a). Knowledge on the origins and characteristics of toxic trace elements such as As, Pb, Cr, Cd, Hg, Se, Sb, Ni, and Tl in feed coal can provide fundamental information for addressing environmental issues and/or human health problems (Dai et al., 2008; Finkelman et al., 2002; Tian et al., 2013).

The physio-chemical properties (e.g. petrography, mineralogy, elemental geochemistry) of coals are dominated by a combination of many geological factors including sediment-source regions, depositional environments, tectonic settings, climate and hydrological conditions etc. (Dai et al., 2015a; Dai et al., 2012b; Li et al., 2014; McCabe, 1991; Querol et al., 1996; Sun et al., 2010a; Swaine, 1990; Swaine and Goodarzi, 1995). Swaine and Goodarzi (1995) indicated that source materials, depositional environments, climatic and hydrological conditions were the dominant factors affecting coal properties. Li et al. (2014) demonstrated that the Early Jurassic coals of Yili basin, Xinjiang Province have contrasting coal qualities between Badaowan Formation and Xishanyao Formation. Dai et al. (2012a, 2012b, 2012c) further summarized and categorized five primary factors for the enrichment of trace elements in Chinese coal deposits: source-rocks (Dai et al., 2008; Dai et al., 2015c; Dai et al., 2013; Dai et al., 2012c), seawater (Liu et al., 2004), volcanic-ash (Dai et al., 2003), hydrothermal-fluid and groundwater (Dai et al., 2012a). In turn, some trace elements are used as geochemical tracers of coal basins. For example, the enrichment of B, Sr, Co, Mo, S and U is commonly used to reflect the degree to which the coal deposits were affected by seawater seawater-influenced coal (Swaine and Goodarzi, 1995).

* Corresponding author at: CAS Key Laboratory of Crust–Mantle Materials and Environment, School of Earth and Space Sciences, University of Science and Technology of China, Hefei, Anhui 230026, China.
E-mail address: lgj@ustc.edu.cn (G. Liu).

http://dx.doi.org/10.1016/j.gexplo.2016.04.002
0375-6742/

Huainan coalfield is situated in the southeastern margin of North China, with abundant coal reserves (Han, 1990; Lan, 1984). Previous studies on the petrology and geochemistry of the regional coals indicated that depositional environment, and epigenetic geological activities (e.g. magmatic intrusion) have significantly affected coal geochemical compositions (Chen et al., 2011; Chen et al., 2014; Sun et al., 2010b; Yang et al., 2012). Additionally, coals from Huainan coalfield are usually transported to other provinces for power generation, which may bring adverse impacts on the environment. Hence, it's essential to investigate the coal quality characteristics and possible geological processes controlling coal quality from both geological and environmental viewpoint.

In this study, we present the data of trace elements in 180 coal samples collected from 9 boreholes in Dingji mine in Huainan coalfield. Our aims are: 1) to assess the concentrations and distribution patterns of the trace elements in coal profiles; 2) to understand the geological processes that affect the geochemical compositions of coals from different coal-forming periods.

2. Geological setting

The Huainan coalfield is situated in southeastern rim of Sino-Korean Platform and is a main Late Paleozoic coal deposition basin of North China (Han, 1990) (Fig. 1). The coalfield is 70 km long (N–S) and 25-km wide (W–E), and covers an area of >2000 km^2, with coal reserves estimated to be approximately 44,000 Mt (Sun et al., 2010a). There are nine active mines in Huainan coalfield and the studied coal mine is located in the central northern part with a length of 13 km (N–S) and width of 11 km in width (E–S) (Fig. 1).

2.1. Coal-bearing strata

The coal-bearing strata in the Huainan coalfield include the Late Carboniferous Taiyuan Formation, the early Permian Shanxi Formation, the Middle Permian Lower Shihezi Formation, and the Late Permian Upper Shihezi Formation. The Taiyuan Formation mainly consists of 13 limestone beds, several layers of mudstone, sandstone and unminable thin coal seams, with an average thickness of ~97 m. There are 29 layers of coal seams in the Shanxi (4.2 m), Lower Shihezi (13.7 m) and Upper Shihezi Formation (9.1 m) with a cumulative thickness of 27 m (Fig. 2). The coal seams of 8, 7-2, 5-1, 4 (split into 4-1, 4-2) in the Lower Shihezi Formation and seams 3, 1 in the Shanxi Formation are sampled in this study. Their total economically minable thickness is ~15 m. Fig. 2 gives a detailed description of stratigraphic and lithological characteristics of coal-bearing sequences.

2.2. Geological process of study area

Previous publications indicated that the coal-bearing sequences in Huainan coalfield were formed on an epicontinental sea, evolving from Shanxi Formation deposited in a tidal-flat delta influenced by brackish water to the Lower Shihezi Formation deposited in a lower delta plain occasionally influenced by seawater incursion (Chen et al., 2011; Lan, 1984; Lan, 1989; Sun et al., 2010a, 2010b; Yang and Lan, 1992). The paleoplate of North China entered the subtropic semiarid and arid climatic belt between the Late Early Permian and Early Late Permian and determined that peat accumulation was restricted to the paralic delta plain where there were oceanic wet climate and high ground water table favoring coal formation (Liu, 1990). From the Early Permian (Shanxi Formation) to the Middle Permian (Lower Shihezi Formation), the subsidence center moved southward to Huainan basin and in turn caused paleoenvironment changes (Han, 1990). The rate of tectonic subsidence in Middle Permian (Lower Shihezi Formation) was relatively higher than the Early Permian (Shanxi Formation), favoring stable accumulation of peat.

3. Materials and methods

During the geological exploration of Dingji mine, a total of 180 coal samples were collected from 9 boreholes of the minable coal seams 1, 3 from Shanxi Formation, seams 4-1, 4-2, 5, 7, 8 from Lower Shihezi Formation. In general, three bench samples are taken from the upper, middle, and lower parts of each coal seam (Fig. 2). All samples were instantly stored in plastic bags to minimize contamination and oxidation.

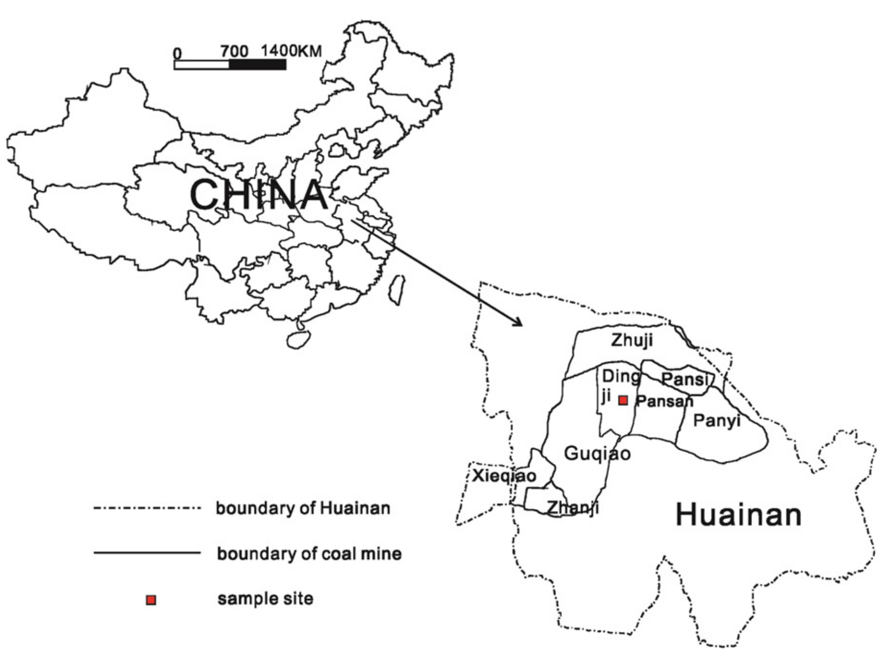

Fig. 1. Location of the Huainan coalfield and main coal mines in the study area.

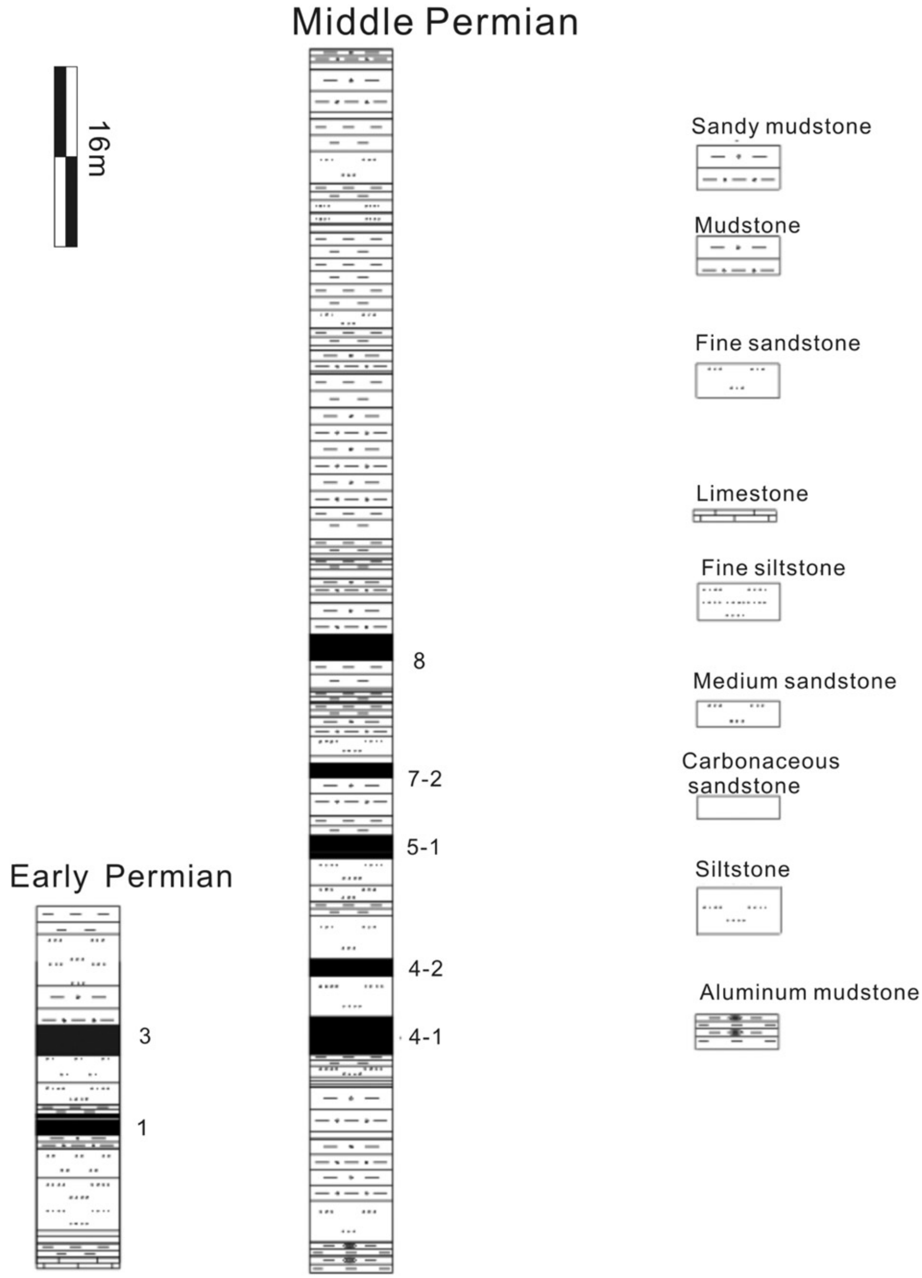

Fig. 2. Stratigraphic column and lithological characteristics of coal-bearing sequence in the Huainan coalfield, Anhui province, China.

The samples were then air-dried, split and ground to pass through 200 mesh sieve before analysis. Coal proximate analysis including moisture, ash yield and volatile matter were determined according to Chinese National Standard GB/T-212 (2008) (comparable to ASTM standards D3173-11-2001 for moisture, D3174-11-2001 for ash yield and D3175-11-2001 for volatile matter). Total sulfur was measured by GB/T-214 (2007) (comparable to ASTM-D4239-12-2012).

The maceral compositions of coal samples were determined by counting points of polished coals under a reflecting microscope according to the Chinese National Standard GB/8899-1998 (comparable to ASTM D2798-11a-2011). Mineralogical analyses of coal samples were performed by X-ray diffraction (XRD, Philips X'Pert PRO), using a target voltage of 40 kV, and an emission current of 30 mA with a scanning angle of 5–70° 2θ at rate of 0.1° per second.

Approximately, 0.1 g of each powder coal sample was weighted by laboratory electronic balance, and then was digested with an acid mixture (HNO_3: HCl: HF = 3:1:1) in a programmed microwave oven (from room temperature to 120 °C in 10 min and kept for 10 min; then increase to 160 °C in 5 min and kept for 10 min; finally increase to 180 °C in 5 min and kept for 15 min). The major elements including Na, Mg, Al, Si, K, Ca, Fe and Ti and trace elements B, Mn, Sr, and Ba, in the coal samples were determined by inductively coupled plasma atomic emission spectrometry (ICP-AES, Optima 7300DV). Other trace elements including Li, Be, Sc, V, Cu, Ni, Zn, As, Pb, Sb, Sn, Cr, Cd, Y, Hf, Th and REE were determined by inductively coupled plasma mass spectrometry (ICP-MS, Thermo X Series 2). The accuracy of the elements was evaluated by the standard reference material NIST-1632b (coal) and GBW07406 (GSS-6, soil). The relative standard deviation was within 5% for most of the elements in replicated samples.

Table 1
The main coal quality parameters of coal seams in Dingji mine, Huainan coalfield.

Coal-bearing strata	Coal seams	Thickness(m)	M_{ad} (%)	A_d (%)	S_{td} (%)	V_{daf} (%)
		Min–max	Min–max	Min–max	Min–max	Min–max
		Ave(N)	Ave(N)	Ave(N)	Ave(N)	Ave(N)
Lower Shihezi Formation	8	0.25–4.84	0.95–4.91	16.66–36.72	0.13–0.79	20.31–40.31
		2.23	1.96(35)	24.32(35)	0.47(30)	35.78(35)
	7-2	0–2.87	0.77–2.90	19.19–38.42	0.25–0.88	9.51–39.30
		0.87	1.71(17)	26.98(17)	0.48(12)	33.97(18)
	5-1	0.83–6.15	0.88–2.68	11.09–28.66	0.29–1.07	30.50–37.27
		3.08	1.77(24)	20.90(25)	0.52(17)	35.80(25)
	4-2	0–4.13	1.09–2.66	16.06–36.37	0.52–1.52	33.78–36.95
		1.56	1.75(20)	25.80(20)	1.00(17)	35.30(19)
Shanxi Formation	4-1	0.33–11.87	1.06–3.56	14.05–25.77	0.23–2.00	30.83–36.31
		3.34	2.06(34)	21.04(34)	0.81(25)	34.60(34)
	3	0.–6.43	1.07–2.45	10.28–31.59	0.23–0.66	32.12–38.10
		2.88	1.70(16)	16.95(16)	0.38(9)	35.23(16)
	1	0–2.13	0.83–2.70	5.33–31.59	0.22–0.83	31.66–39.34
		0.93	1.64(18)	17.20(18)	0.51(9)	34.75(18)

N: the number of samples; Min: minimum; Max: maximum; Ave: average; M_{ad}: moisture on air-dried basis; A_d: ash yields; $S_{t,d}$: total sulfur on dry basis; V_{daf}: volatile matter on dry and ash-free basis.

4. Results and discussion

4.1. Coal quality parameters

The ash yield of coals ranges from 5.33% to 38.42%, with an arithmetic mean of 21.94% (Table 1). Based on the Chinese standard classification for ash yield of coal (GB/T 15224.1-2004 with 10–16% for low ash coal, 16–29% for medium ash coal, and >29% for high ash coal), most samples from the study area are classified as low- to medium-ash coal. Coals from Shanxi Formation (average = 17.08%) are relatively lower in ash yields as compared to coals from Lower Shihezi Formation (average = 23.40%). Sun et al. (2010a, 2010b) also found that ash yields of the coals from Zhuji mine in Huainan coalfield showed the same "increasing stratigraphically upward" trend compared with the coals of Huaibei coalfield (Zheng et al., 2008b); and they ascribed this trend to the increasing terrigenous input igneous intrusion associated with underground water activity within the coal-bearing region. However, coal seams in Dingji mine were rarely affected by igneous intrusion. The relatively high ash yield in the Lower Shihezi Formation coals in the studied area may due to the relatively high accommodation/peat accumulation ratio or high groundwater table of the peat mire favoring minerals accumulation during the Lower Shihezi Formation period (Diessel et al., 2000). In addition, the total sulfur and ash yield is both relatively high in coal seam 4-2 than the split coal seam 4-1.

The major minerals identified by XRD in coal sample include kaolinite, quartz, illite, illite-montmorillonite, montmorillonite and muscovite (Table 2; Fig. 4). As shown in Table 2 and Fig. 3, concentrations of clay minerals in the Lower Shihezi Formation coal are higher than the Shanxi Formation, suggesting clay minerals are mainly derived from detrital debris during the coal formation.

The range of moisture and volatile matter content is 0.77–4.91% and 9.51–40.31%, respectively. According to Chinese National Standards for moisture (MT/850-2000, ≤6.00% for ultra-low moisture coal) and for volatile matter (MT/849-2000, 10–20% for low volatile matter coal, 20–28% for medium volatile coal, 28–37% for medium high volatile coal and 37–50% for high volatile matter coal), the studied coals are classified as ultra-low moisture coal and lower-medium to medium high volatile coal. There is no significant difference in moisture and volatile matter yield between Lower Shihezi Formation (1.89% and 35.16%, respectively) and Shanxi Formation coals (1.67% and 34.89%, respectively).

Table 2 shows the proportions of macerals in coal samples. On average, vitrinite proportion in the Lower Shihezi Formation coals (average = 73%) is higher than Shanxi Formation coals (average = 64%) by 9%, while the inertinite shows a reverse trend. This suggests that the peat in the lower Shihezi Formation was probably formed in a more reducing coal swamp with high water table level (Diessel et al., 2000; Suárez-Ruiz et al., 2012).

It is noted the split coal seams 4-1 and 4-2 exhibit significant difference in maceral composition. As shown in Fig. 3, the contents of vitrinite sharply decrease sharply upward from coal seam 4-1 (average = 79.14%) to 4-2 (average = 63.85%), contrary to the increase of inertinite from coal seam 4-1 (13.96) to 4-2 (24.92%). The variations of ash yield and mineral contents within coal seam 4 show similar trends as inertinite (Fig. 3). Similar trends have been drawn in the Great Northern seam near the top of the Late Permian Newcastle Coal Measures at Wyong, New South Wales, Australia. As shown in

Table 2
The average proportions (%) of macerals and minerals in coal seams from Dingji mine, Huainan coalfield.

Coal seams	Vitrinite	Inertinite	Lipitinite	Organic matter	Clay	Sulfide	Carbonate	Oxides and others	Mineral matters
8	72.9	19.8	7.3	93.4	4.8	0.1	1.7	0.0	6.6
7-2	71.5	19.6	8.9	89.7	8.8	0.3	1.2	0.0	10.3
5-1	75.5	17.4	7.1	95.8	3.2	0.4	0.6	0.0	4.2
4-2	63.9	24.9	11.2	84.9	13.7	1.0	0.4	0.0	12.1
4-1	79.1	14.0	6.9	94.9	4.3	0.3	0.5	0.0	5.1
3	64.7	26.6	8.7	93.6	5.6	0.5	0.3	0.0	6.4
1	63.4	20.3	8.8	91.8	7.1	0.3	0.8	0.0	8.2

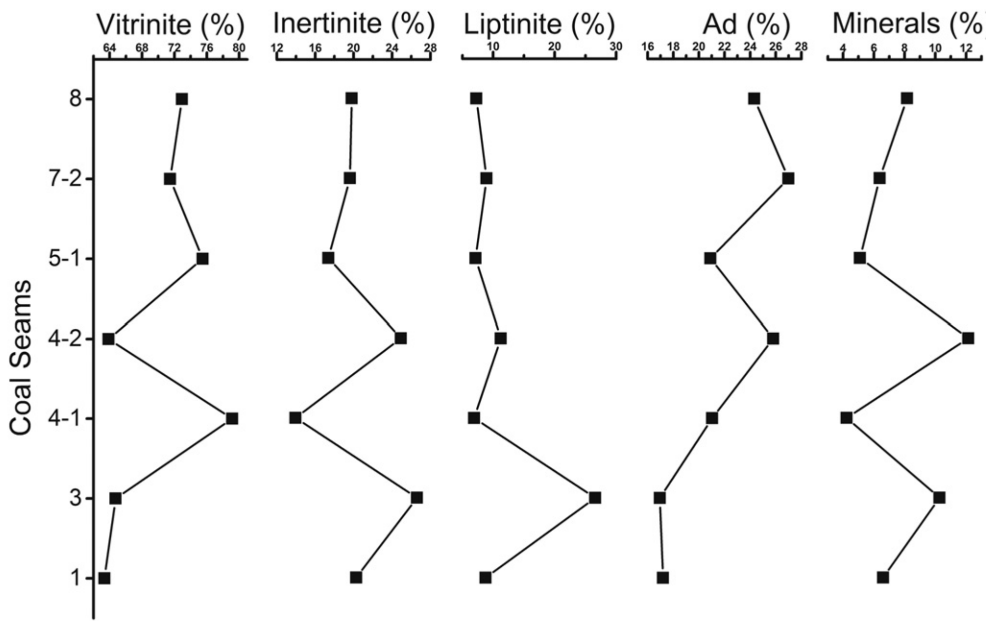

Fig. 3. Vertical variations of vitrinite, inertinite, liptinite proportions, ash yield and mineral contents among coal seams.

some previous studies, split coals with high mineral contents were commonly related to their high peat accommodation/accumulation ratio in the coal basin with more allochthonous coal components, such as detrital minerals (Davies et al., 2005; Diessel, 1992, 2007; Greb et al., 2002). Further, the relatively high accommodation/peat accumulation ratio could result in frequent flooding of the peat which raises the adventitious minerals and generate several thin coal seams (Table 1) in a single stratigraphic sequence (Diessel et al., 2000; Diessel, 2007). The optimum coal-forming conditions require a balanced accommodation/peat accumulation ratio. The shifts of this ratio to other side, i.e. accommodation/peat accumulation ratio >1 or <1, could lead to a deterioration of coal continuity (Diessel et al., 2000; Diessel, 2007; McCabe, 1991). Therefore, due to accelerating basin subsidence since Lower Shihezi Formation, the resultant relatively higher accommodation may contribute to several thin and split coal seams (4-1, 4-2, 5, 7, 8) as shown in Table 1.

4.2. Geochemistry

4.2.1. Element concentrations

Table 3 shows the arithmetic means of major and trace elements for coal seams 1, 3, 4-1, 4-2, 5, 7, and 8 in Dingji mine, Huainan coalfield. Their comparison to the average concentrations of elements in Chinese and world coals is shown in Fig. 5 (Dai et al., 2012a; Ketris and Yudovich, 2009). The Dingji coals are slightly enriched in

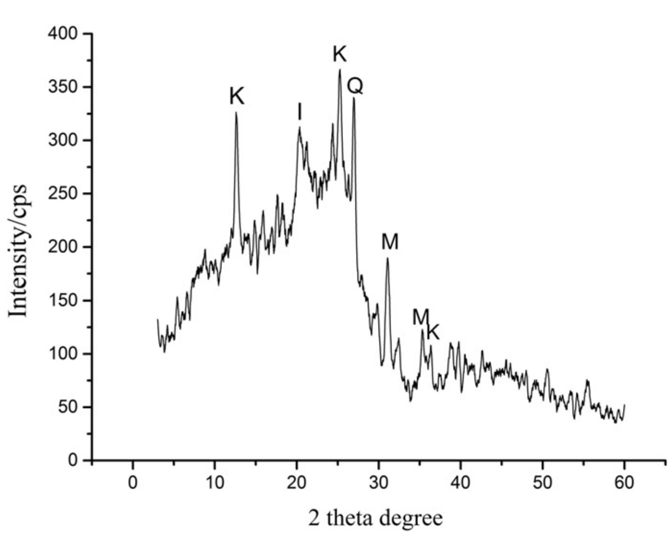

Fig. 4. X-ray diffractogram of selected coal from Dingji Coal Mine: K — kaolinite, I — illite, Q — quartz, M: montmorillonite.

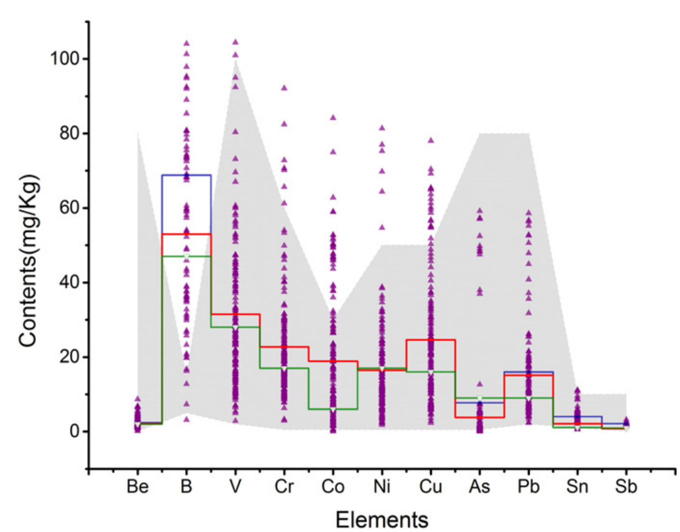

Fig. 5. Variations of potentially hazardous trace elements in Dingji coals. Also shown are the arithmetic averages of potentially hazardous trace elements in world coals (green line), Chinese coals (red line) and Dingji coals (blue line). Shadow area: The range of trace elements concentrations in world coals.

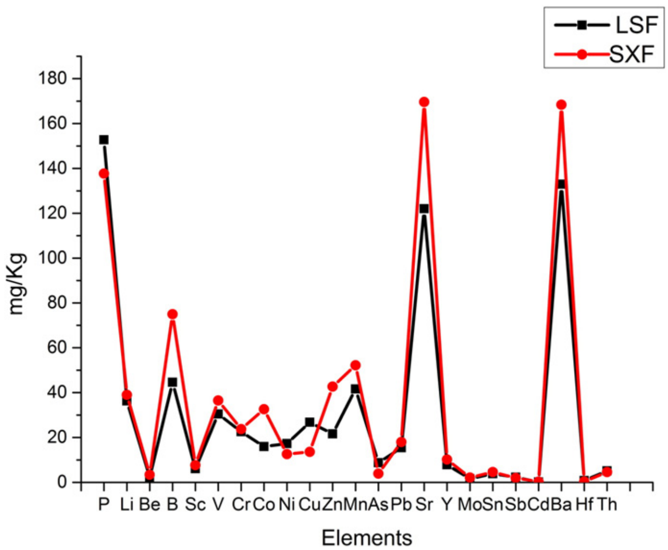

Fig. 6. Variations of trace elements of different formations in Dingji mine, Huainan coalfield. LSF: Lower Shihezi formation; SXF: Shanxi formation.

major elements Al, Na, K and trace elements Li, Be, Sc, Cr, Co, Ni, Cu, As, Pb, Sn and Sb compared to the corresponding elements in Chinese coals reported by Dai et al. (2012a, 2012b, 2012c), and the remainder elements are lower or fairly equal. From the environment point of view, the high abundances of some potentially hazardous trace elements in some coal seams from study area are of great concern. The concentrations of B, V, Cr, Co, Ni, and Cu in some coal samples are above the upper limit of world coals (Ketris and Yudovich, 2009). The arithmetic means of Co, As, Pb, Sn and Sb in Dingji coals are higher than the corresponding elements in Chinese as well as world coals by a factor of 1.5–3.5. Kolker et al. (2009) found that the hazardous trace elements in the abandoned coal mine could be released into surrounding environment, posing great threaten to human health, (Kolker et al., 2009). Therefore, during exploration, transportation and utilization of coals in Dingji mine, great attention should be taken to prevent the release of hazardous trace elements (Co, As, Pb, Sn, Sb) in specific coal seams. (See Table 4.)

The average contents of the trace elements from different coal-bearing formations are shown in Fig. 6. The concentrations of trace elements B, V, Cr, Co, Zn, Mn, Sr and Ba in the coals of Shanxi Formation (coal seams 1 and 3) are higher than those of the Lower Shihezi Formation (coal seams 4-1, 4-2, 5-1, 7-2 and 8). Enrichment of trace elements

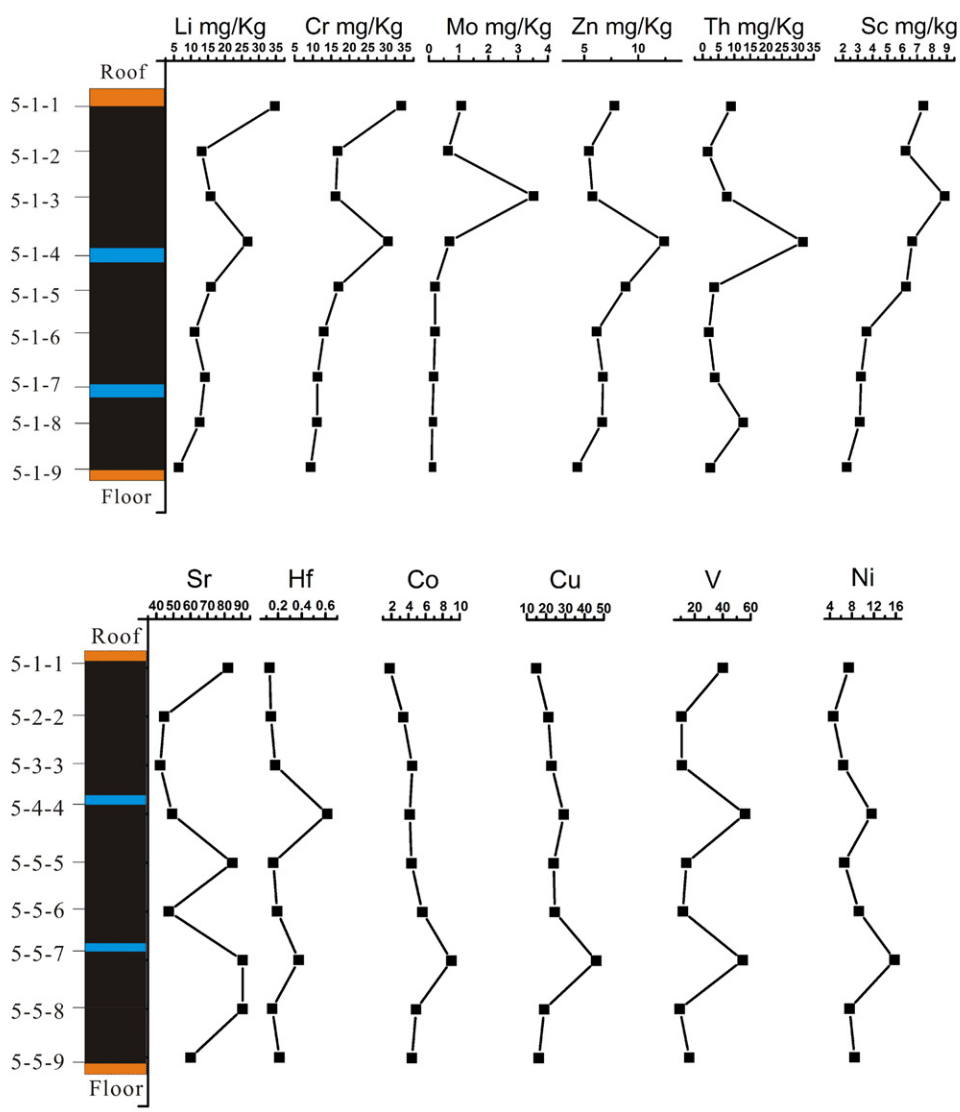

Fig 7. Vertical variations of selected elements in the No. 5-1 coal from borehole DJ2138. Unit for elements: mg/kg.

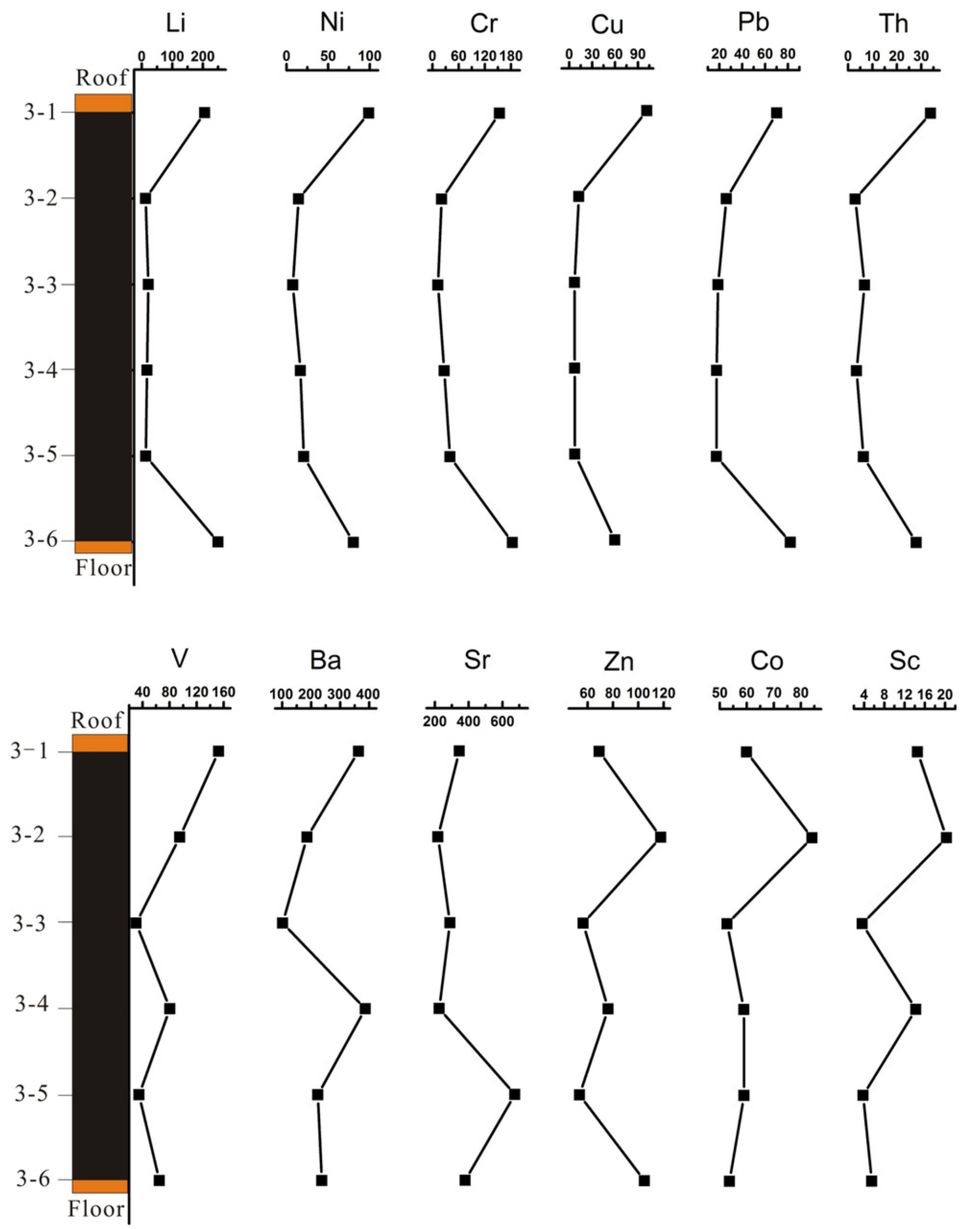

Fig 8. Vertical variations of selected elements in the No. 3 coal from borehole DJ23241; unit for elements: mg/kg.

including B, Sr and Ba is usually indicative of coals deposited in a seawater-influence environment. This is in line with the from previous studies (Chen et al., 2011; Sun et al., 2010b) that indicated that the sweater started to retreat from Huainan coal basin from Early Permian. As shown in Fig. 10, some lithophile elements such as Y, Hf, Si, Al, REE, Ti, P, Th, K and Li are more enriched in Lower Shihezi Formation (coal seams 4-1,4-2, 5-1, 7-2 and 8), which may be attributed to the difference of minerals contents among coal seams. As mentioned above, the accelerating basin subsidence since Lower Shihezi Formation resulted in the paleo-environment changes such as rising groundwater table and increasing detrital input, which may favor minerals formations in some coal seams (4-2, 7-2 and 8) during Lower Shihezi Formation period.

4.2.2. Vertical variations in individual coal seams

The vertical distribution of elements is commonly uneven in individual coal seams (Dai et al., 2015b; Eskenazy, 2009; Hower et al., 2002; Kelloway et al., 2014; Seredin et al., 2006; Yudovich, 2003; Zilbermints et al., 1936), indicating multiple elemental origins and post-depositional processes (Arbuzov et al., 2014; Dai et al., 2014; Permana et al., 2013; Ward, 2002).

In this study, the following coal bench samples were collected to investigate the vertical variation of trace elements in individual coal seams: i) one roof, one floor, two partings and five coal samples of the No. 5-1 coal from borehole DJ2138, and (i) one roof, one floor and four coal samples of the No. 3-1 coal from borehole DJ23241. The distribution patterns of selected trace elements in the No. 5-1 coal from borehole DJ2138 are shown in Fig. 7. Trace elements in this coal seam show large variations. There are increasing trends for Li, Cr, Mo, Zn, Th, Sr and Sc from bottom to the top of the coal seams. Most of the elements (Li, Cr, Zn, Sr, Th, Hf, Co, Cu, V, Ni, V) are enriched in the partings or the coal benches near them, indicating that the partings are significant carriers of these elements. Similar observation, termed as "Zilbermints Law", has been demonstrated by Zilbermints et al. (1936) for Ge in Donetsk

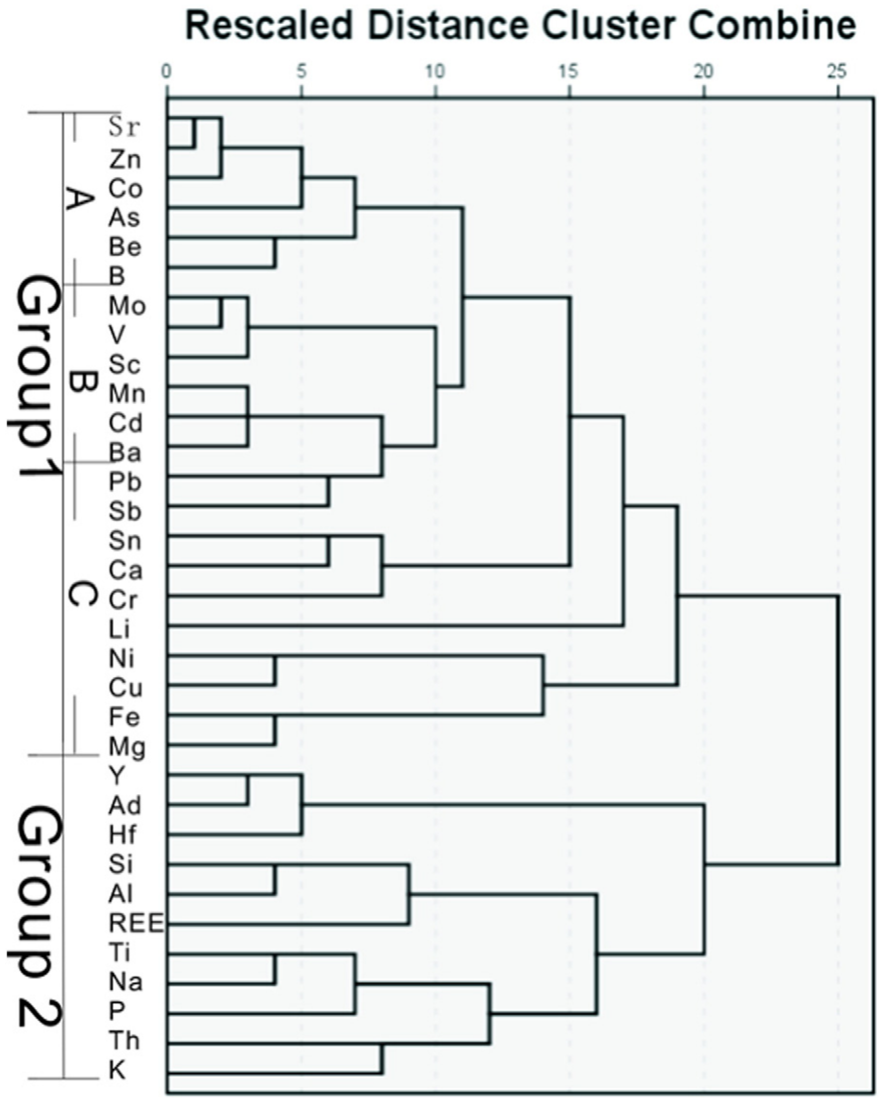

Fig. 9. Dendrogram produced by hierarchical cluster analysis of elemental concentrations among coal seams.

basin coals. Eskenazy (2009) also found that and coal partings have the highest concentrations of Zn, Cr, Co, Ni, and Th.

With regard to the No. 3 coals from borehole DJ 23241, elements including Li, Ni, Cr, Cu, Pb, V and Th show a bow-like distribution pattern, concentrating in the host rocks (roof and floor) (Fig. 8). It possibly indicates that these elements are derived from terrigenous inputs. The uniform variation of these elements in the middle part of the coal bed profile may reflect a relatively stable coal-forming environment. Similar trends have been seen in other studies (Arbuzov et al., 2014; Chen et al., 2015; Chen et al., 2011; Liu et al., 2004; Song et al., 2007). For example, Chen et al. (2015) observed a similar symmetric marginal enrichment of elements in both roof and floor rock samples in the coal seams of Donlin coal mine in Chongqing, southwestern China.

4.2.3. Geochemical associations

The concentrations of trace elements are generally not uniform both laterally and vertically in coal-bearing strata. The vertical variation of trace elements among different coal seams may provide some valuable information with regard to the origins of elements and their relationships with coal-forming environment (Chen et al., 2011; Eskenazy and Stefanova, 2007; Hower et al., 2005; Palmer et al., 2004; Sun et al., 2010b; Zheng et al., 2007; Zheng et al., 2008a).

The vertical distribution patterns of elements among coal seams in stratigraphic units are investigated by hierarchical cluster analysis (Fig. 9). Generally, two groups are classified by cluster analysis.

The elements in Group 1 can be divided into three subgroups: Groups 1A, 1B and 1C (Fig. 10). Trace elements Sr, Zn, Co, As, Be and B are subdivided into Group 1A. Overall, the concentrations of these elements decreased from the lower to upper coal seams (Fig. 10, Group 1). Boron is a good indicator of marine-influenced coals as proposed by Goodarzi and Swaine (Chen et al., 2011; Goodarzi and Swaine, 1994; Liu et al., 2004; Sun et al., 2010b; Yan et al., 2014). In this study, B, Sr, Co, Zn are enriched in coals from Shanxi formation, suggesting that they are possibly brackish seawater origins. This is generally consistent with previous study of Huainan coals (Chen et al., 2011; Lan, 1984; Lan, 1989; Sun et al., 2010b; Yan et al., 2014; Yang and Lan, 1992). Molybdenum, V, Sc, Mn, Cd and Ba are classified into Group 1B (Fig. 10). Almost all these elements are depleted in coal seam 4-2, especially for Mn, Mo, V, Cd. Group 1C is composed of Pb, Sb, Sn, Ca, Cr, Li, Ni, Cu, Fe and Mg (Fig. 10). In general, most of elements in Group 1 are depleted in coal seam 4-2 except for Be, B, Sc, Fe, Mg, Ca, Li and Sn.

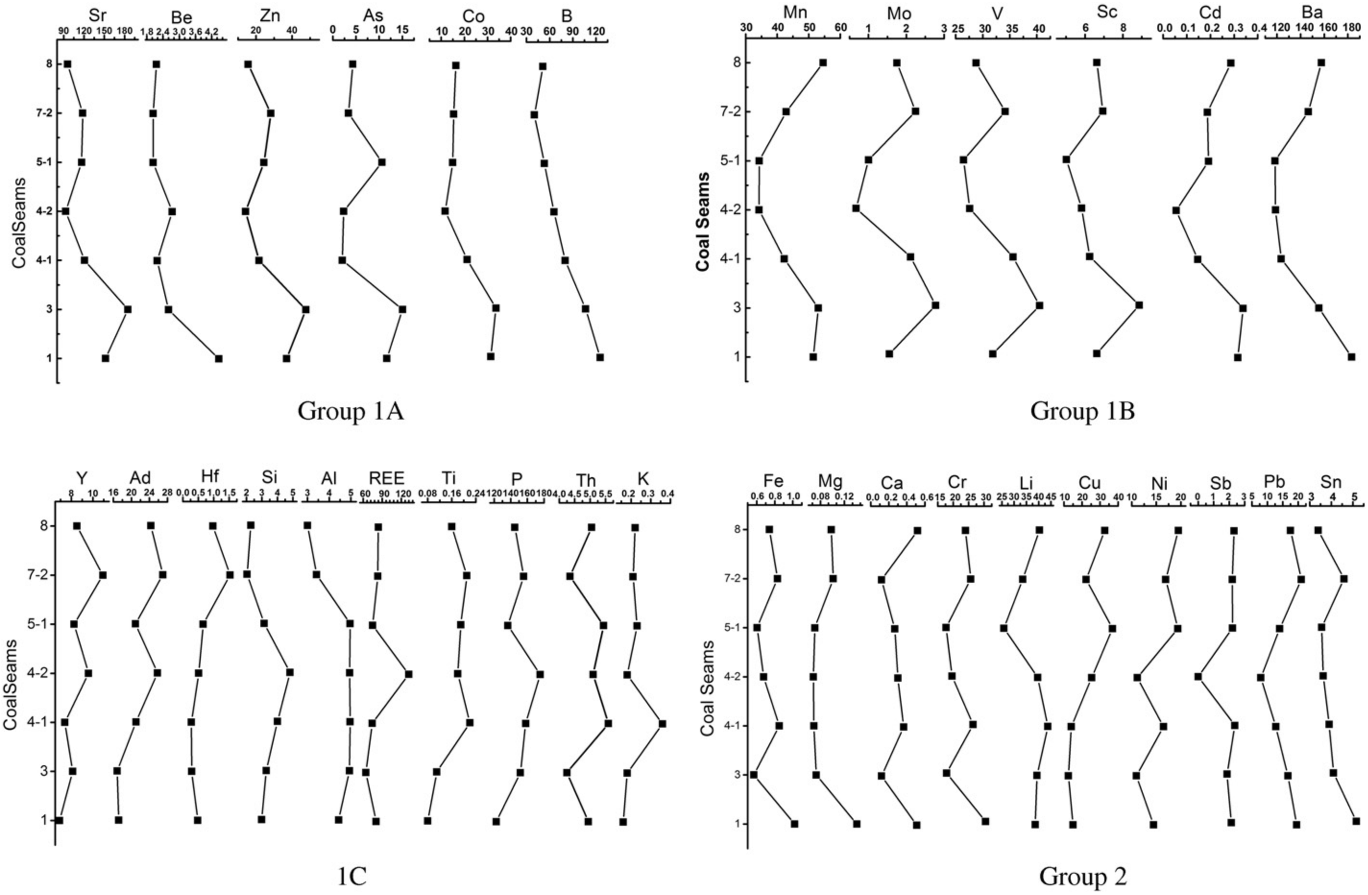

Fig. 10. Vertical variation of elements among 7 mineable coal seams, major elements (Si, Al, Fe, Mg, Na, K, Ca): %; trace elements: mg/kg.

Yttrium, Hf, Si, Al, REE, Ti, P, Th and K are contained in Group 2 (Fig. 10). These elements have high positive correlation coefficients with ash yield. As mentioned above, clay is the primary minerals in coal samples. The vertical distributions of REE, Y, Th and Hf are similar to ash yield, and almost all of them have peak concentrations in coal seam 4-2. In contrast to elements in Group 1A, increased trends in elements concentrations are seen from coal seam 1 to coal seam 8. As mentioned above, Lower Shihezi Formation coal seams might receive the increasing accommodation for peat accumulation may result in relatively more detrital inputs than in Shanxi Formation. More minerals, included kaolinite, illite, montmorillonite that are the host minerals for Si, Hf, Si, Al, REE, Y, Ti, P, Th and K may input into Lower Shihezi coals, especially into coal seam 4-2 and consequently lead to the enrichment of these elements of Group 2 during Lower Shihezi period. Generally, almost all the elements in Group 2 are enriched in coal seam 4-2 as discussed before.

5. Conclusions

In this study, we systematically collected coals from drilling holes in a typical Dingji coal mine, Huainan coalfield, and measured their petrological, mineralogical and geochemical parameters. We found that the average vitrinite contents, ash yields and mineral matters are higher in the Lower Shihezi Formation coals than in the Shanxi Formation coals, suggesting that the upper coal seams were possibly deposited in a more reducing environment with more terrigenous inputs.

A comparison with Chinese coals showed that our studied coals are slightly enriched in major elements Al, Na and K and trace elements Li, Be, Sc, Cr, Co, Ni, Cu, As, Pb, Sn and Sb. The concentrations of potentially hazardous trace elements including Co, As, Pb, Sn and Sb in some coal samples are highly enriched. The vertical variations of trace elements within individual coal seams indicate that host rocks are carriers of some elements in coal. Using hierarchical cluster analysis, we broadly classified two groups of elements. Group 1 includes three subgroups of 1A (Sr–Zn–Co–As–Be–B), 1B (Mo–V–Sc–Mn–Cd–Ba–Pb–Sb) and 1C (Sn–Ca–Cr–Li–Ni–Cu–Fe–Mg). Group 2 has a typical elemental combination of Y–Hf–Si–Al–REE–Ti–P–Th–K. Most of elements in Group 1 are depleted in coal seam 4-2, whereas most elements in Group 2 are enriched in coal seam 4-2.

Acknowledgments

This work was supported by the National Basic Research Program of China (973 Program, 2014CB238903), the National Natural Science Foundation of China (41373110 and 41402133), We acknowledge editors and reviewers for polishing the language of the paper and for in-depth discussion.

Appendix A. Supplementary data

Supplementary data to this article can be found online at http://dx.doi.org/10.1016/j.gexplo.2016.04.002.

Table 3
The numbers of samples, and abundances of 47 elements in coal seams.

Elements	8				7-2				5-1				4-2				4-1				3				1			
	Average	Max	Min	N	Average	Max	Min	N	Average	Max	Min	N	Average	Max	Min	N	Average	Max	Min	N	Average	Max	Min	N	Average	Max	Min	N
SiO_2%	4.87	12.57	0.23	16	4.37	12.50	0.77	13	6.73	17.97	1.28	11	10.31	20.29	1.83	5	8.58	18.64	2.50	11	7.03	13.83	0.66	9	6.37	16.54	1.49	11
TiO_2%	0.27	1.06	0.02	29	0.35	1.21	0.02	29	0.32	1.24	0.02	34	0.31	0.81	0.03	19	0.37	0.98	0.06	27	0.18	0.57	0.02	18	0.13	0.49	0.03	19
Al_2O_3%	5.68	14.24	1.10	22	6.47	14.12	1.28	17	9.24	16.13	0.94	14	9.71	15.91	1.87	10	9.34	15.86	1.60	16	9.33	24.19	1.38	11	8.40	20.73	0.76	11
Fe_2O_3%	1.46	3.34	0.16	28	0.81	1.50	0.25	19	1.22	15.63	0.25	33	0.97	2.16	0.44	10	0.86	1.34	0.51	19	1.12	2.38	0.11	13	1.06	2.64	0.35	14
MgO%	0.23	0.63	0.03	26	0.12	0.26	0.03	26	0.11	0.30	0.01	33	0.11	0.36	0.02	19	0.12	0.27	0.01	25	0.17	0.33	0.04	18	0.16	0.38	0.06	19
CaO%	0.17	0.31	0.10	12	0.72	1.20	0.23	12	0.51	1.64	0.07	21	0.42	1.18	0.07	12	0.37	0.68	0.07	11	0.17	0.32	0.06	9	0.73	1.84	0.02	12
Na_2O%	0.42	0.87	0.04	5	0.33	0.43	0.27	3	0.54	0.65	0.39	4	0.60	0.88	0.33	3	0.61	0.91	0.35	3	0.34	0.51	0.24	3	bdl	bdl	bdl	0
K_2O%	0.26	1.09	0.02	14	0.25	0.71	0.04	15	0.27	1.16	0.04	16	0.22	1.03	0.02	12	0.43	0.89	0.06	11	0.21	0.39	0.03	9	0.19	0.57	0.02	13
P	144.89	422.64	38.05	14	155.56	492.83	33.87	17	136.46	283.84	39.87	16	175.34	382.87	58.75	10	157.99	388.80	49.83	19	151.61	291.73	36.44	12	122.55	233.05	34.24	11
Li	40.37	89.35	17.37	21	33.54	78.03	9.83	21	25.83	74.94	10.84	26	39.64	96.44	13.50	17	43.73	93.83	12.78	25	39.34	67.02	12.65	15	38.61	68.89	13.27	13
Be	2.16	6.34	1.27	16	2.03	4.00	0.83	18	2.04	4.93	1.20	27	2.74	6.63	1.28	14	2.18	6.76	0.93	14	2.60	8.68	0.14	12	4.46	5.56	3.27	7
B	51.24	92.49	7.28	14	40.18	85.38	3.15	15	53.08	75.54	12.74	17	65.54	175.12	16.26	8	80.19	164.37	20.51	17	106.56	249.23	45.92	10	125.52	146.10	67.43	7
Sc	6.63	9.94	3.24	21	6.94	12.70	3.18	18	5.02	9.29	1.04	25	5.82	8.05	2.57	12	6.25	10.41	3.52	19	8.87	20.26	2.44	12	6.63	1.00	2.33	13
V	28.77	73.15	2.83	29	34.16	104.42	4.92	29	26.47	135.42	6.97	35	27.59	92.42	10.11	17	35.61	100.97	14.29	25	40.53	94.99	8.44	15	31.86	60.62	6.52	13
Cr	24.02	47.03	12.50	28	25.68	82.43	3.28	29	17.69	47.37	6.30	36	19.64	53.31	8.56	17	26.43	92.11	2.93	24	17.87	40.12	7.85	15	30.51	61.21	13.17	13
Co	16.36	51.85	0.02	28	15.41	49.86	0.50	29	14.96	47.07	0.20	36	11.73	32.32	0.61	17	21.16	51.42	2.46	22	33.62	84.14	1.51	15	31.41	74.95	5.59	13
Ni	19.49	64.40	7.82	28	16.92	81.38	3.83	29	19.40	77.00	3.57	36	11.13	23.31	1.78	17	16.47	38.74	2.30	25	10.95	21.73	2.91	15	14.46	38.43	6.62	13
Cu	25.42	40.53	10.95	28	22.32	56.48	6.17	29	36.98	78.02	4.80	37	14.97	35.11	5.72	12	14.02	26.24	2.33	24	12.48	44.10	4.89	15	32.68	70.37	4.48	17
Zn	15.59	67.17	8.89	27	28.20	69.80	3.75	29	24.36	87.84	2.70	36	14.16	38.84	3.54	17	21.63	89.63	4.34	25	47.63	117.79	3.98	15	36.96	103.96	8.15	13
Mn	54.61	5.75	267.66	26	42.87	10.83	115.10	26	34.27	6.19	85.96	33	34.20	3.02	111.16	19	42.25	3.54	103.74	26	53.03	3.33	110.42	18	51.43	9.42	231.51	19
As	4.31	7.15	0.23	10	3.36	7.45	0.64	8	10.59	48.37	0.38	16	2.33	7.64	0.36	8	2.04	5.29	0.03	16	15.04	59.16	0.57	14	11.66	52.45	0.03	14
Pb	17.50	56.69	4.08	21	21.01	58.58	2.42	17	14.01	52.77	2.31	23	7.92	14.93	5.04	9	12.75	26.17	4.80	14	16.66	26.19	9.04	12	19.52	40.80	6.67	10
Sr	95.67	275.10	26.75	28	118.09	552.09	19.83	29	116.42	617.18	20.83	36	92.9133	403.681	11.82	17	120.73	893.81	10.67	25	185.08	673.40	38.21	15	151.80	310.25	57.43	13
Y	8.51	21.02	0.58	29	10.92	21.70	5.27	29	8.26	19.40	1.02	37	9.59	21.56	2.83	15	7.40	16.52	0.74	25	8.12	19.93	1.75	16	6.91	17.40	0.93	13
Mo	1.75	5.05	0.04	15	2.25	5.94	0.48	14	1.00	3.22	0.11	19	0.67	2.52	0.04	9	2.11	11.56	0.27	14	2.77	16.94	0.10	9	1.55	4.46	0.23	10
Sn	3.39	5.37	0.53	8	4.59	10.67	0.82	14	3.55	6.75	0.83	17	3.63	5.47	0.53	8	3.90	5.68	1.73	14	4.10	5.02	1.92	10	5.16	9.54	1.33	8
Sb	2.31	2.47	2.23	3	2.21	2.26	2.17	3	2.22	2.25	2.16	3	bdl	bdl	bdl	0	2.37	2.68	2.20	3	1.86	2.24	1.49	7	2.14	3.17	1.80	5
Cd	0.29	0.57	0.06	9	0.19	0.40	0.04	11	0.19	0.40	0.02	11	0.05	0.11	0.02	9	0.15	0.40	0.01	11	0.34	0.49	0.03	12	0.32	0.82	0.03	9
Ba	157.62	404.59	31.16	25	146.61	521.00	37.60	29	118.37	263.29	45.74	37	118.83	283.69	49.19	17	123.62	203.32	34.18	25	155.54	386.67	39.70	15	183.24	372.71	77.52	13
La	16.15	45.15	0.14	28	11.58	37.30	0.36	29	13.13	73.81	0.32	37	14.71	142.42	1.03	17	11.75	35.39	0.03	25	15.80	31.30	0.83	15	32.87	94.40	2.67	10
Ce	35.58	91.97	1.39	29	24.31	58.23	0.83	29	36.49	162.45	2.75	37	29.93	87.84	3.76	17	34.43	68.28	3.93	25	35.75	59.73	14.70	15	49.31	101.62	22.53	13
Pr	4.43	12.67	1.45	19	5.61	10.91	0.52	16	5.81	10.70	1.46	21	5.11	9.04	1.10	8	5.23	9.56	1.77	14	4.66	8.72	1.88	12	4.89	11.78	1.53	9
Nd	13.31	39.64	1.49	29	9.94	23.99	0.87	29	12.50	51.56	1.53	37	11.84	98.94	0.84	17	10.57	27.87	1.05	25	12.20	25.63	0.83	15	25.44	94.65	3.02	13
Sm	4.47	11.22	2.23	20	2.77	4.70	0.90	18	3.19	8.49	0.59	23	3.33	17.00	0.42	9	3.54	7.80	0.78	14	3.80	6.93	1.33	12	7.24	16.64	2.01	10
Eu	1.00	2.52	0.37	19	0.90	1.52	0.21	16	0.68	1.48	0.15	21	0.75	3.57	0.15	9	1.06	2.04	0.21	14	1.16	2.05	0.24	12	1.70	4.15	0.48	10
Gd	2.67	8.00	0.42	26	1.72	3.55	0.27	26	1.93	5.95	0.31	35	1.85	10.94	0.23	17	2.00	5.23	0.24	25	2.62	5.51	0.63	15	3.28	9.56	0.20	13
Tb	0.56	1.72	0.21	18	0.52	1.20	0.09	16	0.70	2.18	0.23	21	0.68	1.76	0.23	9	0.62	1.61	0.10	14	0.64	1.46	0.11	12	0.63	1.81	0.16	10
Dy	2.30	9.58	0.94	27	3.47	6.06	1.42	27	3.17	7.22	0.86	35	2.95	9.64	0.64	17	2.18	5.80	0.80	25	2.23	4.76	0.75	15	2.46	6.08	0.58	13
Ho	0.55	1.40	0.27	19	0.54	0.92	0.20	16	0.45	0.97	0.14	21	0.44	0.89	0.30	9	0.62	1.18	0.27	14	0.66	1.22	0.16	12	0.79	1.25	0.29	10
Er	0.96	2.84	0.29	27	1.02	1.92	0.21	27	0.95	1.68	0.28	35	0.88	1.70	0.28	17	1.09	2.09	0.23	25	1.22	2.64	0.39	15	1.10	2.34	0.29	13
Tm	0.23	0.66	0.09	19	0.29	1.00	0.09	16	0.20	0.59	0.06	21	0.31	0.96	0.09	12	0.31	0.57	0.10	14	0.31	0.63	0.06	12	0.34	0.77	0.10	10
Yb	1.30	3.69	0.32	28	1.33	3.41	0.29	29	0.90	3.08	0.27	37	1.01	1.58	0.53	17	1.28	3.16	0.28	25	1.78	3.98	0.32	15	1.58	4.24	0.54	13
Lu	0.40	0.94	0.12	27	0.38	0.98	0.02	27	0.36	1.13	0.06	35	0.37	0.83	0.15	17	0.26	0.98	0.11	25	0.15	0.31	0.08	15	0.25	0.69	0.10	13
REE	74.18	387.11	9.75		64.38	155.67	6.28		80.47	331.29	9.00		131.89	349.98	34.48		74.94	171.56	9.88		83.00	154.87	22.31		83.91	231.99	9.73	
Hf	0.97	3.90	0.14	14	1.53	9.00	0.17	12	0.66	5.20	0.07	20	0.52	1.70	0.08	9	0.28	0.61	0.17	8	0.29	0.35	0.26	5	0.48	0.83	0.31	5
Th	5.05	10.36	2.27	18	4.35	11.85	0.91	16	5.44	20.80	1.09	27	5.10	9.41	2.70	9	5.59	10.89	1.23	14	4.25	8.34	0.75	12	4.94	9.87	1.32	10

bdl: below detection limit; Max: maximum; Min: minimum; N: the number of coal samples. The unit for major element oxides is % and for other elements is mg/kg.

Table 4
The elemental abundances in coals from the Dingji coal mine and comparisons with Chinese and world coals.

Elements	This study				Chinese coals[a]		World coals		
	Max	Min	AM	N	AM	N	Max	Min[b]	AM[c]
SiO_2%	20.29	0.24	4.71	76	8.47	1322	nd	nd	nd
TiO_2%	1.24	0.017	0.28	175	0.33	1322	nd	nd	0.133
Al_2O_3%	24.19	0.76	7.88	97	5.98	1322	nd	nd	nd
Fe_2O_3%	15.63	0.11	1.13	136	4.85	1322	nd	nd	nd
MgO%	0.63	0.008	0.15	166	0.22	1322	nd	nd	nd
CaO%	1.83	0.014	0.48	85	1.23	1322	nd	nd	nd
Na_2O%	0.9	0.04	0.47	21	0.16	1322	nd	nd	nd
K_2O%	1.16	0.01	0.27	90	0.19	1322	nd	nd	nd
P	492.83	33.87	149.28	99	400	1322	10	1	3.9
Li	96.44	9.83	36.83	138	31.8	1274	80	1	14
Be	8.68	0.14	2.4	108	2.11	1249	15	0.1	2
B	155.77	3.15	50.46	88	53	1048	400	5	47
Sc	20.26	1.04	6.42	120	4.38	1919	10	1	3.7
V	135.42	2.83	31.49	163	35.1	1324	100	2	28
Cr	92.11	2.93	22.76	162	15.4	1615	60	0.5	17
Co	84.14	0.02	18.88	160	7.08	1523	30	0.5	6
Ni	81.38	1.78	16.49	163	13.7	1392	50	0.5	17
Cu	78.02	2.33	24.61	162	17.5	1362	50	0.5	16
Zn	117.79	2.7	25.26	162	41.4	1458	300	5	28
Ga	136.2	1	19.55	87	6.55	2451	20	1	5.8
Mn	267.66	3.02	43.98	167	116	1322	300	5	71
As	59.16	0.03	7.73	86	3.79	3386	80	0.5	9
Pb	58.58	2.31	15.96	106	15.1	1446	80	2	9
Sr	893.81	10.67	130.19	163	140	2075	500	15	10
Y	21.7	0.58	8.25	164	18.2	888	50	2	8.2
Mo	16.94	0.04	1.7	90	3.08	789	10	0.1	2.2
Sn	10.67	0.53	4.02	79	2.11	848	10	1	1.1
Sb	3.17	bdl	2.13	24	0.84	596	10	0.1	0.9
Cd	0.82	0.01	0.22	72	0.25	1384	3	0.1	0.2
Ba	521	31.16	139.12	161	159	1205	300	70	150
La	142.42	0.03	14.81	161	22.5	392	40	11	1
Ce	162.45	0.83	34.14	165	46.7	392	70	2	23
Pr	12.67	0.52	5.15	99	6.42	392	10	1	3.4
Nd	98.94	0.83	12.82	165	22.3	392	30	3	12
Sm	17	0.42	3.87	106	4.07	392	6	0.5	2.2
Eu	4.15	0.15	0.99	101	0.84	392	2	0.1	0.43
Gd	10.94	0.2	2.2	157	4.65	392	4	0.4	2.7
Tb	2.18	0.09	0.62	100	0.62	392	1	0.1	0.31
Dy	9.64	0.58	2.75	159	3.74	392	4	0.5	2.1
Ho	1.4	0.14	0.56	101	0.96	392	2	0.1	0.57
Er	2.84	0.21	1.01	159	1.79	392	3	0.5	1
Tm	1	0.06	0.27	104	0.64	392	nd	nd	0.3
Yb	4.24	0.27	1.25	164	2.08	392	3	0.3	1
Lu	1.13	0.02	0.33	159	0.38	392	1	0.03	0.2
Hf	9	0.07	0.77	73	3.71	392	5	0.5	1.2
Th	20.8	0.75	5.02	106	5.84	1052	10	0.5	3.2

Max: maximum; Min: minimum; AM: arithmetic average; N: the number of coal samples; nd: no data; the unit for major element oxides is % and for other elements is mg/kg.
[a] From Dai et al. (2012a).
[b] From Swaine (1990).
[c] From Ketris and Yudovich (2009).

References

Arbuzov, S.I., Volostnov, A., Mezhibor, A.M., Rybalko, V., Ilenok, S., 2014. Scandium (Sc) geochemistry in coals (Siberia, Russian Far East, Mongolia, Kazakhstan, and Iran). Int. J. Coal Geol. 125, 22–35.

BP report. BP statistical Review of World Energy, 2015. http://www.bp.com/en/global/corporate/energy-economics/statistical-review-of-world-energy/coal-review-by-energy-type.html.

Chen, J., Chen, P., Yao, D., Liu, Z., Wu, Y., Liu, W., Hu, Y., 2015. Mineralogy and geochemistry of Late Permian coals from the Donglin Coal Mine in the Nantong coalfield in Chongqing, southwestern China. Int. J. Coal Geol. 149, 24–40.

Chen, J., Liu, G., Jiang, M., Chou, C.-L., Li, H., Wu, B., Zheng, L., Jiang, D., 2011. Geochemistry of environmentally sensitive trace elements in Permian coals from the Huainan coalfield, Anhui, China. Int. J. Coal Geol. 88, 41–54.

Chen, J., Liu, G., Li, H., Wu, B., 2014. Mineralogical and geochemical responses of coal to igneous intrusion in the Pansan Coal Mine of the Huainan coalfield, Anhui, China. Int. J. Coal Geol. 124, 11–35.

Dai, S., Li, T., Seredin, V.V., Ward, C.R., Hower, J.C., Zhou, Y., Zhang, M., Song, X., Song, W., Zhao, C., 2014. Origin of minerals and elements in the Late Permian coals, tonsteins, and host rocks of the Xinde Mine, Xuanwei, eastern Yunnan, China. Int. J. Coal Geol. 121, 53–78.

Dai, S., Ren, D., Chou, C.-L., Finkelman, R.B., Seredin, V.V., Zhou, Y., 2012a. Geochemistry of trace elements in Chinese coals: a review of abundances, genetic types, impacts on human health, and industrial utilization. Int. J. Coal Geol. 94, 3–21.

Dai, S., Ren, D., Hou, X., Shao, L., 2003. Geochemical and mineralogical anomalies of the late Permian coal in the Zhijin coalfield of southwest China and their volcanic origin. Int. J. Coal Geol. 55, 117–138.

Dai, S., Seredin, V.V., Ward, C.R., Hower, J.C., Xing, Y., Zhang, W., Song, W., Wang, P., 2015a. Enrichment of U–Se–Mo–Re–V in coals preserved within marine carbonate successions: geochemical and mineralogical data from the Late Permian Guiding Coalfield, Guizhou, China. Mineral. Deposita 50, 159–186.

Dai, S., Tian, L., Chou, C.-L., Zhou, Y., Zhang, M., Zhao, L., Wang, J., Yang, Z., Cao, H., Ren, D., 2008. Mineralogical and compositional characteristics of Late Permian coals from an area of high lung cancer rate in Xuan Wei, Yunnan, China: Occurrence and origin of quartz and chamosite. Int. J. Coal Geol. 76, 318–327.

Dai, S., Wang, P., Ward, C.R., Tang, Y., Song, X., Jiang, J., Hower, J.C., Li, T., Seredin, V.V., Wagner, N.J., 2015b. Elemental and mineralogical anomalies in the coal-hosted Ge ore deposit of Lincang, Yunnan, southwestern China: Key role of N_2 – CO_2 -mixed hydrothermal solutions. Int. J. Coal Geol. 152, 19–46.

Dai, S., Wang, X., Seredin, V.V., Hower, J.C., Ward, C.R., O'Keefe, J.M.K., Huang, W., Li, T., Li, X., Liu, H., Xue, W., Zhao, L., 2012b. Petrology, mineralogy, and geochemistry of the Ge-rich coal from the Wulantuga Ge ore deposit, Inner Mongolia, China: New data and genetic implications. Int. J. Coal Geol. 90–91, 72–99.

Dai, S., Yang, J., Ward, C.R., Hower, J.C., Liu, H., Garrison, T.M., French, D., O'Keefe, J.M., 2015c. Geochemical and mineralogical evidence for a coal-hosted uranium deposit in the Yili Basin, Xinjiang, northwestern China. Ore Geol. Rev. 70, 1–30.

Dai, S., Zhang, W., Ward, C.R., Seredin, V.V., Hower, J.C., Li, X., Song, W., Wang, X., Kang, H., Zheng, L., 2013. Mineralogical and geochemical anomalies of late Permian coals from the Fusui Coalfield, Guangxi Province, southern China: influences of terrigenous materials and hydrothermal fluids. Int. J. Coal Geol. 105, 60–84.

Dai, S., Zou, J., Jiang, Y., Ward, C.R., Wang, X., Li, T., Xue, W., Liu, S., Tian, H., Sun, X., 2012c. Mineralogical and geochemical compositions of the Pennsylvanian coal in the Adaohai Mine, Daqingshan Coalfield, Inner Mongolia, China: modes of occurrence and origin of diaspore, gorceixite, and ammonian illite. Int. J. Coal Geol. 94, 250–270.

Davies, R., Diessel, C., Howell, J., Flint, S., Boyd, R., 2005. Vertical and lateral variation in the petrography of the Upper Cretaceous Sunnyside coal of eastern Utah, USA—implications for the recognition of high-resolution accommodation changes in paralic coal seams. Int. J. Coal Geol. 61, 13–33.

Diessel, C., Boyd, R., Wadsworth, J., Leckie, D., Chalmers, G., 2000. On balanced and unbalanced accommodation/peat accumulation ratios in the Cretaceous coals from Gates Formation, Western Canada, and their sequence-stratigraphic significance. Int. J. Coal Geol. 43, 143–186.

Diessel, C.F., 1992. Coal Formation and Sequence Stratigraphy. Springer.

Diessel, C.F., 2007. Utility of coal petrology for sequence-stratigraphic analysis. Int. J. Coal Geol. 70, 3–34.

Eskenazy, G.M., 2009. Trace elements geochemistry of the Dobrudza coal basin, Bulgaria. Int. J. Coal Geol. 78, 192–200.

Eskenazy, G.M., Stefanova, Y.S., 2007. Trace elements in the Goze Delchev coal deposit, Bulgaria. Int. J. Coal Geol. 72, 257–267.

Finkelman, R.B., Belkin, H.E., Zheng, B., 1999. Health impacts of domestic coal use in China. Proc. Natl. Acad. Sci. 96, 3427–3431.

Finkelman, R.B., Orem, W., Castranova, V., Tatu, C.A., Belkin, H.E., Zheng, B., Lerch, H.E., Maharaj, S.V., Bates, A.L., 2002. Health impacts of coal and coal use: possible solutions. Int. J. Coal Geol. 50, 425–443.

Goodarzi, F., Swaine, D.J., 1994. The influence of geological factors on the concentration of Boron in Australian and Canadian Coals. Chem. Geol. 118, 301–318.

Greb, S., Eble, C., Hower, J., Andrews, W., 2002. Multiple-bench architecture and interpretations of original mire phases—examples from the Middle Pennsylvanian of the Central Appalachian Basin, USA. Int. J. Coal Geol. 49, 147–175.

Han, S., 1990. Coal-forming Conditions and Coalfield Prediction in Huaibei-Huainan Region. Geological Publishing House, Beijing, China (in Chinese with English abstract).

Hower, J.C., Eble, C.F., Quick, J.C., 2005. Mercury in Eastern Kentucky coals: geologic aspects and possible reduction strategies. Int. J. Coal Geol. 62, 223–236.

Hower, J.C., Ruppert, L.F., Williams, D.A., 2002. Controls on boron and germanium distribution in the low-sulfur Amos coal bed, Western Kentucky coalfield, USA. Int. J. Coal Geol. 53, 27–42.

Kelloway, S.J., Ward, C.R., Marjo, C.E., Wainwright, I.E., Cohen, D.R., 2014. Quantitative chemical profiling of coal using core-scanning X-ray fluorescence techniques. Int. J. Coal Geol. 128, 55–67.

Ketris, M., Yudovich, Y.E., 2009. Estimations of Clarkes for Carbonaceous biolithes: world averages for trace element contents in black shales and coals. Int. J. Coal Geol. 78, 135–148.

Kolker, A., Panov, B.S., Panov, Y.B., Landa, E.R., Conko, K.M., Korchemagin, V.A., Shendrik, T., McCord, J.D., 2009. Mercury and trace element contents of Donbas coals and associated mine water in the vicinity of Donetsk, Ukraine. Int. J. Coal Geol. 79, 83–91.

Lan, C., 1984. The sedimentary environment of the coal-bearing formation of the Permian period in the Huainan coalfield. J. Anhui Univ. Sci. Technol. 2, 10–22 (in Chinese with English abstract).

Lan, C., 1989. Sedimentary characteristics and environments of Carboniferous–Permian coal-bearing rock formations in Huainan–Huaibei coalfields. J. Huainan Min. Inst. 3, 9–22 (in Chinese with English abstract).

Li, B., Zhuang, X., Li, J., Zhao, S., 2014. Geological controls on coal quality of the Yili Basin, Xinjiang, Northwest China. Int. J. Coal Geol. 131, 186–199.

Li, S., Xiao, T., Zheng, B., 2012. Medical geology of arsenic, selenium and thallium in China. Sci. Total Environ. 421–422, 31–40.

Liu, G., 1990. Permo-Carboniferous paleogeography and coal accumulation and their tectonic control in the North and South China continental plates. Int. J. Coal Geol. 16, 73–117.
Liu, G., Yang, P., Peng, Z., Chou, C.-L., 2004. Petrographic and geochemical contrasts and environmentally significant trace elements in marine-influenced coal seams, Yanzhou mining area, China. J. Asian Earth Sci. 23, 491–506.
Liu, G., Zheng, L., Duzgoren-Aydin, N.S., Gao, L., Liu, J., Peng, Z., 2007a. Health effects of arsenic, fluorine, and selenium from indoor burning of Chinese coal. Reviews of Environmental Contamination and Toxicology. Springer, pp. 89–106.
Liu, G., Zheng, L., Gao, L., Zhang, H., Peng, Z., 2005. The characterization of coal quality from the Jining coalfield. Energy 30, 1903–1914.
Liu, G., Zheng, L., Zhang, Y., Qi, C., Chen, Y., Peng, Z., 2007b. Distribution and mode of occurrence of As, Hg and Se and Sulfur in coal Seam 3 of the Shanxi Formation,Yanzhou Coalfield, China. Int. J. Coal Geol. 71, 371–385.
McCabe, P., 1991. Tectonic controls on coal accumulation. Bull. Soc. Geol. Fr. 162, 277–282.
Palmer, C.A., Tuncalı, E., Dennen, K.O., Coburn, T.C., Finkelman, R.B., 2004. Characterization of Turkish coals: a nationwide perspective. Int. J. Coal Geol. 60, 85–115.
Permana, A.K., Ward, C.R., Li, Z., Gurba, L.W., 2013. Distribution and origin of minerals in high-rank coals of the South Walker Creek area, Bowen Basin, Australia. Int. J. Coal Geol. 116, 185–207.
Qi, C., Wu, F., Deng, Q., Liu, G., Mo, C., Liu, B., Zhu, J., 2011. Distribution and accumulation of antimony in plants in the super-large Sb deposit areas, China. Microchem. J. 97, 44–51.
Querol, X., Cabrera, L., Pickel, W., López-Soler, A., Hagemann, H., Fernández-Turiel, J., 1996. Geological controls on the coal quality of the Mequinenza subbituminous coal deposit, northeast Spain. Int. J. Coal Geol. 29, 67–91.
Seredin, V., Danilcheva, Y.A., Magazina, L., Sharova, I., 2006. Ge-bearing coals of the Luzanovka Graben, Pavlovka brown coal deposit, southern Primorye. Lithol. Miner. Resour. 41, 280–301.
Song, D., Qin, Y., Zhang, J., Wang, W., Zheng, C., 2007. Concentration and distribution of trace elements in some coals from Northern China. Int. J. Coal Geol. 69, 179–191.
Suárez-Ruiz, I., Flores, D., Mendonça Filho, J.G., Hackley, P.C., 2012. Review and update of the applications of organic petrology: Part 1, geological applications. Int. J. Coal Geol. 99, 54–112.
Sun, R., Liu, G., Zheng, L., Chou, C.-L., 2010a. Characteristics of coal quality and their relationship with coal-forming environment: a case study from the Zhuji exploration area, Huainan coalfield, Anhui, China. Energy 35, 423–435.
Sun, R., Liu, G., Zheng, L., Chou, C.-L., 2010b. Geochemistry of trace elements in coals from the Zhuji Mine, Huainan Coalfield, Anhui, China. Int. J. Coal Geol. 81, 81–96.
Swaine, D.J., 1990. Trace elements in coal. Butterworth-Heinemann 27–49.
Swaine, D.J., Goodarzi, F., 1995. Environmental aspects of trace elements in coal. Energy Environ. 2, 2.
Tian, H., Lu, L., Hao, J., Gao, J., Cheng, K., Liu, K., Qiu, P., Zhu, C., 2013. A review of key hazardous trace elements in Chinese coals: abundance, occurrence, behavior during coal combustion and their environmental impacts. Energy Fuel 27, 601–614.
Ward, C.R., 2002. Analysis and significance of mineral matter in coal seams. Int. J. Coal Geol. 50, 135–168.
Yan, Z., Liu, G., Sun, R., Wu, D., Wu, B., Zhou, C., Tang, Q., Chen, J., 2014. Geochemistry of trace elements in coals from the Huainan Coalfield, Anhui, China. Geochem. J. 48, 331–344.
Yang, M., Liu, G., Sun, R., Chou, C.-L., Zheng, L., 2012. Characterization of intrusive rocks and REE geochemistry of coals from the Zhuji Coal Mine, Huainan Coalfield, Anhui, China. Int. J. Coal Geol. 94, 283–295.
Yang, S., Lan, C., 1992. The depositional environment of Yinfeng district, Huainan coalfield. Coal Geol. China 4, 6–9 (in Chinese with English abstract).
Yudovich, Y.E., 2003. Notes on the marginal enrichment of germanium in coal beds. Int. J. Coal Geol. 56, 223–232.
Zheng, L., Liu, G., Chou, C.-L., 2007. The distribution, occurrence and environmental effect of mercury in Chinese coals. Sci. Total Environ. 384, 374–383.
Zheng, L., Liu, G., Qi, C., Zhang, Y., Wong, M., 2008a. The use of sequential extraction to determine the distribution and modes of occurrence of mercury in Permian Huaibei coal, Anhui Province, China. Int. J. Coal Geol. 73, 139–155.
Zheng, L., Liu, G., Wang, L., Chou, C.-L., 2008b. Composition and quality of coals in the Huaibei Coalfield, Anhui, China. J. Geochem. Explor. 97, 59–68.
Zilbermints, V., Rusanov, A., Kosrykin, V., 1936. On the question of Ge-presence in fossil coals. Acad. VI Vernadsky—k 169–190.